ORIENTAL JOURNAL OF CHEMISTRY
An International Open Access, Peer Reviewed Research Journal
www.orientjchem.org
ISSN: 0970-020 X
CODEN: OJCHEG
2025, Vol. 41, No.(6):
Pg. 1942-1955

Pristimerin Suppresses STAT3 Signaling in Colorectal Cancer Cells by Targeting JAK2: *In silico* and *In vitro* Evidence

BASHIR A. YOUSEF[1,2*], MUHANAD ELHAFIZ[3], ELSAMOUAL IBRAHIM AHMEDANI[4], MOHAMMED ISMAIL[5], AMAL A. BAHAFI[6], MOHAMED A. EL-MOSELHY[1,7], and MOHAMMED ALSAYED SALEH[8,9]

[1*]Department of Clinical Pharmacy and Pharmacology, IbnSina National College for Medical Studies, Jeddah, Saudi Arabia.
[2]Department of Pharmacology, Faculty of Pharmacy, University of Khartoum, Khartoum, Sudan.
[3]Department of Pharmacology, Faculty of Pharmacy, Omdurman Islamic University, Khartoum, Sudan.
[4]Department of Pathology and Microbiology, IbnSina National College of Medical Studies, Jeddah, Saudi Arabia.
[5]Department of Pharmacology, Faculty of Medicine and Health Science, Dongola University, Dongola, Sudan.
[6]Department of Pharmaceutical Sciences, IbnSina National College of Medical Studies, Jeddah, Saudi Arabia.
[7]Department of Pharmacology and Toxicology, Faculty of Pharmacy, Minia University, Minya, Egypt.
[8]Department of Biophysiology, IbnSina National College of Medical Studies, Jeddah, Saudi Arabia.
[9]Department of Physiology, Faculty of Medicine, Cairo University, Cairo, Egypt.
*Corresponding author E-mail: bashiralsiddiq@gmail.com

http://dx.doi.org/10.13005/ojc/410609

(Received: October 11, 2025; Accepted: November 28, 2025)

ABSTRACT

This study investigated the molecular mechanisms underlying the anticancer effects of pristimerin, a natural triterpenoid, against colorectal cancer (CRC) through modulation of the STAT3 signaling pathway. Using *in vitro* assays in HCT-116 cells and *in silico* modeling, the cytotoxic, molecular, and dynamic effects of pristimerin were evaluated. The MTT assay revealed that pristimerin significantly reduced the viability of CRC cells in a dose-dependent manner. Western blot analysis demonstrated potent inhibition of STAT3 phosphorylation. Molecular docking indicated a strong binding affinity of pristimerin for Janus kinase 2 (JAK2), suggesting that its inhibitory effect on STAT3 activation occurs through upstream JAK2 blockade. Molecular dynamics simulations further confirmed the stability of the pristimerin–JAK2 complex, supporting a direct inhibitory mechanism. Collectively, these results highlight pristimerin's ability to suppress CRC cell growth by targeting the JAK2/STAT3 axis, providing a mechanistic rationale for its development as a potential therapeutic agent in colorectal cancer.

Keywords: Pristimerin, Colorectal cancer, JAK2, STAT3, Molecular dynamics.

INTRODUCTION

Colorectal cancer (CRC) is a common cancer with a wide global burden. It is classified as the second most common type of malignancy in females and the third most common type of cancer in males[1]. Universally, CRC also shows high mortality rates and is considered a principal death cause among cancer types[2]. The WHO documented approximately 935,000 deaths from CRC worldwide in 2020[3]. CRC is a multifactorial disease characterized by a range of abnormalities at the genetic and epigenetic levels that affect a variety of signaling pathways responsible for the development of CRC hallmarks[4,5]. Signal Transducer and Activator of Transcription 3 (STAT3) signaling pathway is one of the molecular pathways that have been involved in CRC carcinogenesis[6,7]. STAT3 functions as a key oncogenic transcription factor that promotes cell-cycle progression, inhibits apoptosis, and drives angiogenesis and metastasis. Additionally, STAT3 contributes to immune evasion by inducing immunosuppressive mediators and plays a major role in mediating chemoresistance in colorectal cancer[8-12].

STAT3 is a downstream target at the Tyrosine kinase receptor (TKR) signaling pathway that mediates the action of fibroblast growth factor, epidermal growth factor, vascular endothelial growth factor, and several interleukins, including interferon-γ, IL-6, and IL-10[13]. STAT3 structure consists of 770 amino acids that form six domains or motifs including the N-terminal domain (NTD) including residues 1-138, the coiled-coil domain (CCD) which includes residues 139-320, the DNA-binding domain (DBD) containing residues 321-494, the linker domain (LD) with the residues 495-583, the Src homology 2 (SH2) with the residues 584-688, and lastly the transactivation domain (TAD) with the residues 689-77014. Activation of STAT3 required phosphorylation at Tyrosine 705, which is located in the TAD, followed by dimerization of the phosphorylated STAT3 at SH2 domain. Ser727 is another phosphorylation site located at TAD, which enhances STAT3 target gene transcription. STAT3 Tyr705 phosphorylation can take place as a result of direct activation of kinases associated with TKRs, including Janus kinase 2 (JAK2) and Tyrosine kinase 2 (TYK2), where the Src-Ras pathway is responsible for Ser727 phosphorylation through the activation of JNK, P38, or ERK1/2[15].

As natural compounds are more tolerant of the human body, they have gained importance in the creation of new anticancer drugs[16]. Pristimerin is a natural triterpenoid that is recovered from the *Celastraceae* and *Hippocrateaceae* families. It has long been used as an anti-inflammatory, antioxidant, and insecticidal agent[17,18]. Pristimerin has been reported to exhibit anticancer activities against various cancer cell types[19]. These antitumor activities are referred to its effect on different signaling pathways in cancer cells and affecting various cancer hallmarks[20]. Furthermore, pristimerin was reported to have anticancer activity against CRC cells, it induced apoptosis, suppressed cell growth, angiogenesis, and metastasis in different CRC cell lines[21-23].

Given STAT3's central role in CRC progression and chemoresistance, it represents an attractive therapeutic target for novel anticancer strategies[24]. Although pristimerin has been shown to interfere with several oncogenic pathways, its direct influence on STAT3 signaling and upstream kinase regulation in CRC remains insufficiently characterized. Therefore, this study aimed to comprehensively investigate the anticancer effects of pristimerin in colorectal cancer by examining its impact on STAT3 activation through integrated in vitro experiments and in silico molecular modeling approaches.

MATERIALS AND METHODS

Materials

Pristimerin (Fig. 1A) was obtained from Xingda Biotechnology (Guangzhou, China). MTT from Sigma (St. Louis, MO, USA). Antibodies against STAT3, p-STAT3, and β-actin were from Santa Cruz Biotechnology (Santa Cruz, CA, USA). Anti-mouse IgG-horseradish peroxidase was purchased from KangChen Biotechnology (Shanghai, China).

In vitro studies

Cell lines and cell culture

HCT-116 was purchased from the

American Type Culture Collection (ATCC). Cells were cultured in RPMI 1640 medium (HyClone China Ltd., China) that contained 10% fetal bovine serum (Gibco-BRL, Grand Island, NY, USA), penicillin (100 U/mL), and streptomycin (100 µg/mL) (Sigma, St. Louis, MO, USA) and incubated at 37°C in a humidified atmosphere containing 5% CO_2.

Cell viability assay

MTT assay was applied to assess pristimerin's inhibitory effect on HCT-116 cells. Briefly, $5x10^3$ cells/well were seeded into a 96-well plate for one day, thenthe cells were treated with pristimerin for 48 hours. Following treatment, MTT (0.5 mg/mL) was added to each well for 4 hours. Then, 150µL DMSO was added to solubilize the insoluble formazan crystals, and absorbance was measured using a microplate reader at 540 nm. Viability % was measured using this equation = (Absorbance of treated-well)/(Absorbance of non-treated well) x 100. Then, the inhibition rate% (IR%) was calculated (IR% = 100-Viability%).

Western blot analysis

HCT-116 cells were treated with pristimerin for 48 h, then the cells were collected and lysed using lysis buffer (Vazyme Biotech Co., LTD, Nanjing, China). Then, the cells were centrifuged for 15 min at 12,000 rpm and 4°C. The supernatant total protein was measured using Bicinchoninic acid (BCA) protein assay kit (Beyotime Institute of Biotechnology, Nanjing, China). The protein was separated using SDS-PAGE with 80V for 30 min and at 120V for 1.5 h and ran for 45 min to transfer the protein into a nitrocellulose membrane. The membrane was blocked using TBST buffer containing 5% free-fat milk for 2 h with gentle shaking. Then, the membrane was incubated with a gentle shaking with the designated primary antibodies at 4°C overnight. The membrane was washed with TBST to remove the excess antibody and incubated with the secondary antibodies at room temperature for 2 hours. Finally, the membrane was washed again with TBST buffer, visualized using chemiluminescence detection kit, and scanned using a ChemiDoc XRS imaging system.

***In silico* studies**

Software

For this study, Flare™, version 6.1.0, Cresset®, Litlington, Cambridgeshire, UK was utilized for molecular docking and visualization of ligand-protein complex[25-27], where GROMACS, Version 2023.2, was used for molecular dynamics studies[28].

Protein and Ligands Preparation

Crystallographic structure for JAK1 kinase domain (JH1) with co-crystallized compound (PDB:5E1E)[29], and kinase domain (JH1) of JAK2 in complex with its inhibitor Fedratinib (PDB: 7VNE)[30], was recovered from the Protein Data Bank (PDB)[31]. Flare Protein Prep tool was used to extract the co-crystallized ligand, missing hydrogenswere added, the active site was determined based on the co-crystallized ligand, and grid was set to 6°C. Finally, the receptor protein was minimized using Normal Open MM calculation, and charges were assigned using AM1-BCC model. Pristimerin and Baricitinib 3D structure was retrieved from the PubChemdatabase, striped of salts, and pH was set at 7 using Flare Ligand Prep wizard and minimized using the Accurate XED model.

Molecular Docking

Flare software was used to perform the docking. The designated compounds were docked into the targeted protein using the normal dock function of Flare; in addition to that, the co-crystallized ligands were re-docked to validate the results.

Molecular Dynamic (MD) Simulations

The preferred pose of pristimerin and Fedratinib, which was obtained from the docking, were further subjected to MD simulations to validate the stability, conformational flexibility, and binding efficacy of the ligand-protein complex. In the beginning, the missing residues in JAK2 protein and missing hydrogen were added using SWISS-MODEL server[32], then the protein was prepared using dock prep tool of UCSF chimera version 1.17.133. All-atom MD simulations were conducted using GROMACS, and the compound's topologies were created using SwissParam server[34]. CHARMM36 (MacKerell lab) force field and modified TIP3P water model were applied

to perform MD simulation of all complexes. All simulations were conducted in a triclinic box with the protein centered at 1nm from the edge. The complexes were neutralized using the appropriate number of ions. Following that, the protein was minimized to resolve clashes and bad connections. Then, two steps of equilibration were conducted, NVT equilibration of 100 ps, and NPT equilibration with a similar time. The system temperature was maintained at 300 k using V-rescale, a modified Berendsen thermostat, where the pressure was maintained by using Parrinello-Rahman barostat at 1 atm. Finally, MD simulations were carried out for 100 ns, with a time step of 2 fs. Further analysis of Structural and conformational in the systems was performed using various GROMACS analysis modules. Data were visualized using Xmgrace software.

Molecular Mechanics-based Poisson Boltzmann Surface Area (MMPBSA) calculations

To estimate the free binding energy from the last 10 ns of the simulation 100 equilibrated frames at 100 ps intervals were utilized, and the following equation was used to calculate the net free energy of the binding:

$$\Delta G \text{ binding} = G \text{ complex} - (G \text{ protein} + G \text{ Ligand})$$

The estimation of the binding free energy for the ligand-protein complexes was conducted using the MMPBSA approach with the gmx_ MMPBSA tool[35,36], which utilizes an integrated Adaptive Poisson-Boltzmann Solver (APBS) tool to calculate the electrostatic energy, van der Waals energy, and polar solvation energy contributions[37]. Where the non-polar energy contribution was estimated based on the Solvent-accessible surface area (SASA). Finally, Energy decomposition per residue was conducted for all complexes to highlight the key interaction residues[38]. Adaptive Poisson-Boltzmann Solver (APBS) tool to calculate the electrostatic energy, van der Waals energy, and polar solvation energy contributions[37]. Where the non-polar energy contribution was estimated based on the Solvent-accessible surface area (SASA). Finally, Energy decomposition per residue was conducted for all complexes to highlight the key interaction residues[38].

Principal component analysis (PCA) and Gibbs free energy landscape (FEL) analysis

Generally, PCA is a multivariate statistical method utilized to build a covariance matrix containing fewer variables from a large data set which explains the whole data set and enables its visualization and analysis, where the method can be applied to explain the collective atomic motion and the conformational changes in proteins[39,40]. PCA was used to examine the C^4 fluctuations and the associated change in the protein configuration following the ligand binding at the last 50 ns of the simulation with reference to the apoprotein. The covariance matrix was constructed via gmxcovar tool of gromacs to calculate the eigenvector and eigenvalue which indicated the direction of $C\alpha$ motion and the value of the motion, respectively. The first three eigenvalue known as principal component 1 (PC1), PC2 and PC3 were utilized to represent the collective motion as it contains 70-90% of the total contribution of the atomic motion[41,42]. To build the 2D projection of $C\alpha$ motion, we used gmxanaeig tool of gromacs. Finally, Gibbs free energy landscape analysis was conducted using MD DaVis tool to establish the energy changes in relation to the conformational change and compare the energy minima upon the binding of the ligands, where RMSD of ligands fit to protein and radius of gyration of the complexes were used to create the free energy landscape, then the metastable conformations were extracted from the trajectories and visualized using Flare software.

Statistical analysis

Data were analyzed using GraphPad Prism 6 (GraphPad Software, Inc., San Diego, CA, USA). Data were expressed as mean±standard deviation (SD) for three independent experiments. All figures are derived from our original experimental and computational results. Statistical differences between treated and untreated cells were assessed by a two-tailed Student's test. p-value<0.05 was considered statistically significant.

RESULTS

Pristimerin inhibited cellular growth in HCT-116 cells

Pristimerin provoked significant dose-

dependent inhibition of HCT-116 cell viability. Following 48 h of treatment, the IC_{50}% value was 1.22±0.25 µM (Fig. 1(b)), which indicates pristimerin has potent cytotoxic effects against CRC cells.

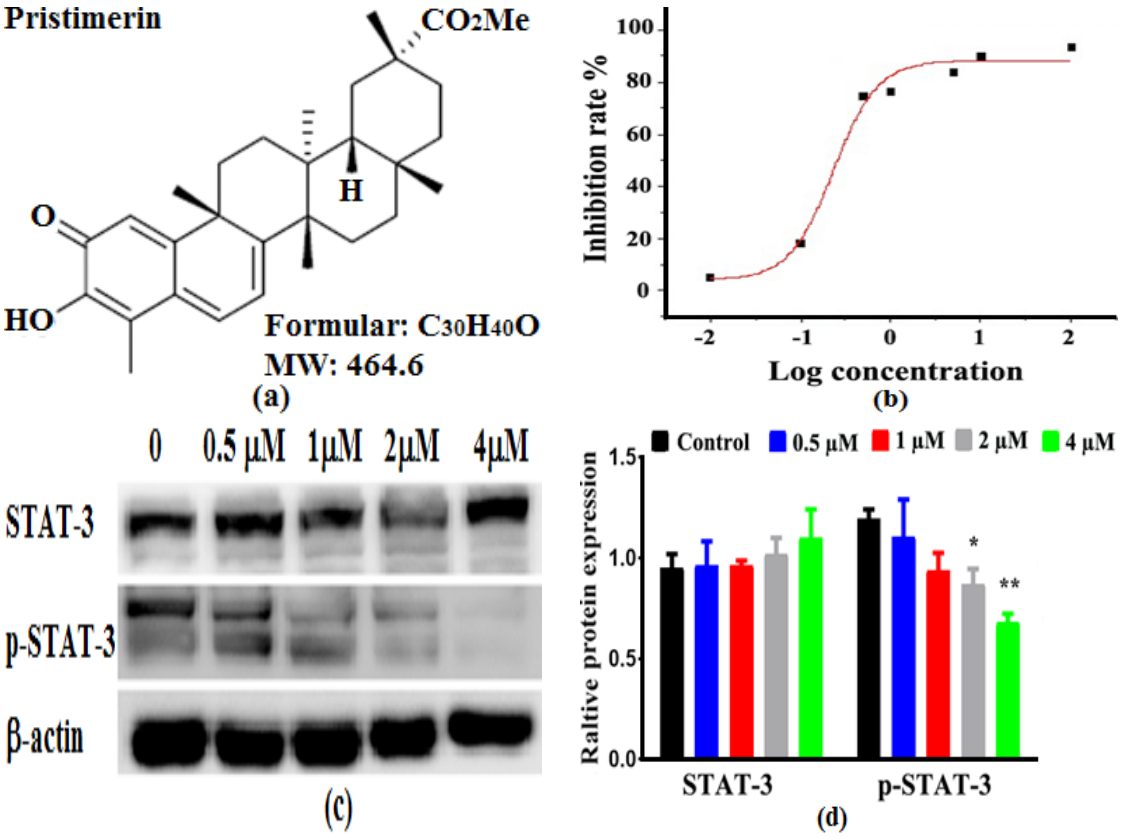

Fig 1(a) Pristimerin chemical structure. (b) Effect of pristimerin on HCT-116 cell viability. IC_{50}% was calculated using dose-response curve for measurement of inhibition rate % for cells treated with pristimerin for 48 h using MTT assay. (c) Effect of pristimerin on SATT3 signaling pathway, cells were treated with pristimerin for 48 h, total cell lysates were analyzed by western blot analysis for STAT-3 and p-STAT-3 proteins, β-actin was used as the control. (d) Quantifications of relative protein expression of these proteins were measured. Data were represented as mean±SD from three independent experiments. *p<0.05, **p<0.01 pristimerin versus control

Pristimerin exhibits an inhibitory effect on STAT3 phosphorylation in HCT-116 cells

We examined whether pristimerin effect on HCT-116 cancer cells is related to the expression and activation of STAT3. As shown in Fig. 1(c) and 1(d), pristimerin demonstrated mild and insignificant suppressive action on STAT3 total protein expression in HCT-116 cells, accompanied by a significant reduction in the phosphorylation of STAT3 at Tyr705 in a concentration-dependent manner, which revealed pristimerin ability to inhibit STAT3 phosphorylation and eventually its activation.

Pristimerin is a potential selective JAK2 inhibitor

To determine how Pristimerin reduces the phosphorylation of STAT3, we investigated the possible interaction of pristimerin with upstream kinases responsible of STAT3 phosphorylation at Tyr705. For that, we picked JAK1, JAK2 for further investigation using molecular docking as they are responsible for the phosphorylation of STAT3 at Tyr705, and due to their authenticated role in CRC development.

Molecular Docking

The docking results for the selected compounds with JAK2 are summarized in Table 1. FLARE, using the Lead Finder approach for docking and scoring[43], evaluates each compound using three scores: the rank score, which predicts the accuracy of the 3D pose; the dG score, which estimates the binding affinity of the ligand to the protein; and the VS score, which differentiates between true and false binders[44].

Table 1: Docking score and estimated free binding energy of selected compounds with targets

Docking score of selected compounds with JAK1 and JAK2			
JAK1	Rank score	dG score	VS score
Pristimerin	-5.873	-7.522	-8.088
Baricitinib	-8.901	-8.895	-11.702
JAK2			
Pristimerin	-9.063	-10.021	-10.616
Fedratinib	-9.331	-11.105	-12.027

Estimated free binding energy using molecular mechanics/Poisson–Boltzmann surface area approach					
	ΔVDWAALS	ΔEEL	ΔENPOLAR	ΔEPB	ΔTOTAL
Pristimerin	-46.23	-26.96	4.71	57.42	-20.47
Fedratinib	-62.07	-18.18	-6.21	84.06	-2.40

ΔVDWAALS = Delta van der waals forces, ΔEEL= Delta electrostatic energy, Delta non polar solvation energy, ΔEPB= Delta polar solvation energy.

Compared to baricitinib, a pan-JAK inhibitor, pristimerin exhibited a low binding affinity to JAK1, with an unfavorable pose and a suboptimal total virtual screening score. These results indicate that pristimerin is not a JAK1 inhibitor. In contrast, docking studies for both pristimerin and fedratinib with JAK2 showed considerable rank, dG, and VS scores for both compounds, with fedratinib showing superior scores relative to pristimerin. It is noteworthy that fedratinib is an FDA-approved selective JAK2 inhibitor. The comparable docking score of pristimerin to fedratinib with JAK2 prompted us to focus on the interaction of pristimerin with JAK2. Fedratinib interacts with JAK2 through three strong hydrogen bonds with Leu855 and Leu932, along with multiple hydrophobic interactions with Val863, Leu855, Ala880, Val911, Met929, and Leu983 (Fig. 2(b)). In contrast, pristimerin forms a strong hydrogen bond with Phe860 and a weak hydrogen bond with Gly861, in addition to multiple hydrophobic interactions with Val863 and Asp994 (Figure 2(a)).

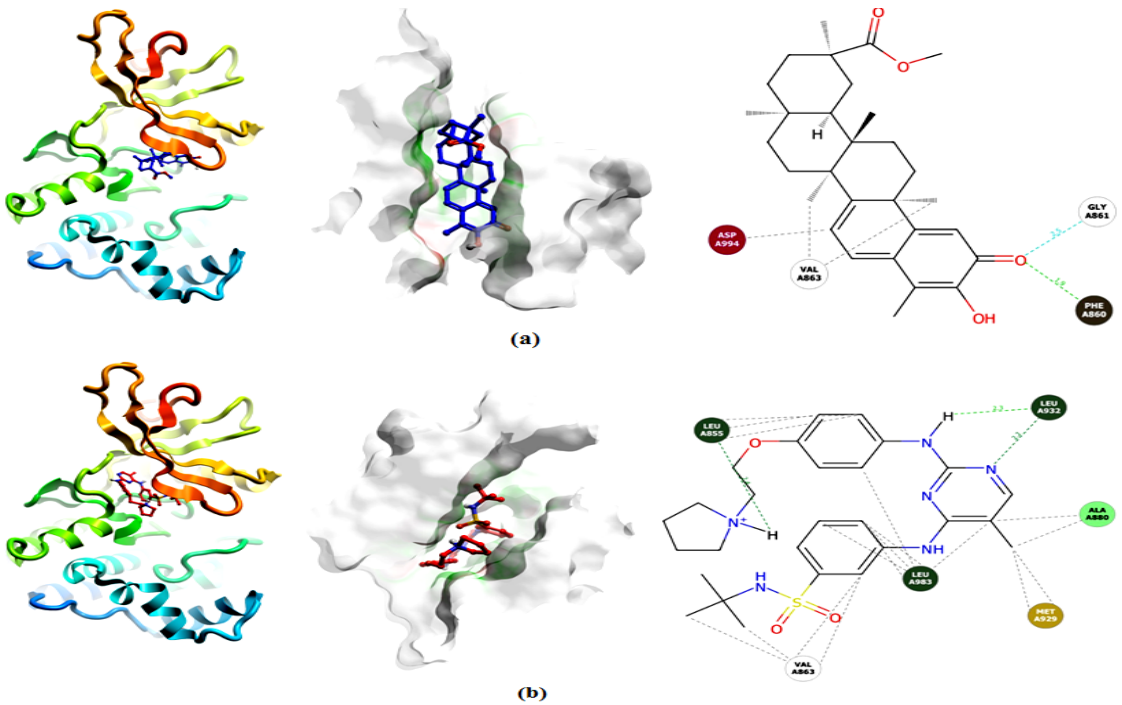

Fig. 2. Attained pose andinteraction map for (a)Pristimerin, (b) Fedratinib with JAK2 following molecular docking using flare software

Molecular Dynamics (MD) Simulation Analysis

To assess the stability of the pristimerin-JAK2 complex and examine the accuracy of the docking-predicted pose, we employed Molecular Dynamics (MD) simulations. The stability of the complex indicated that the interaction is feasible at the biological level[45]. The Root Mean Square Deviation (RMSD) of the ligand-protein complex was used to evaluate the stability of the system during the simulation. A smaller RMSD deviation after the conformational change, when the ligand binds to the receptor, reflects a higher stability of the complex. Additionally, we monitored the Cα RMSD throughout the MD simulation to determine whether the receptor reached a stable state while maintaining the ligand-protein interaction. The Root Mean Square Fluctuation (RMSF) per residue was used to assess the flexibility of protein regions in response to ligand binding.

Furthermore, we employed the Radius of Gyration (Rg) to evaluate the compactness of the complex and protein folding upon ligand binding. A lower Rg value with minimal fluctuation indicates proper protein folding and stable conformation, whereas a higher Rg value suggests misfolding and instability[46]. Finally, we used the Solvent Accessible Surface Area (SASA) to estimate the area of the complex exposed to the solvent. A higher SASA might affect ligand-protein interactions due to increased exposure to the aqueous environment, potentially impacting the folding of hydrophobic regions of the protein[47].

RMSD, RMSF, Rg, and SASA Analysis

Analysis of the RMSD for the pristimerin-JAK2 complex showed that the RMSD remained stable at 2 Å throughout the simulation, while the RMSD of the fedratinib-JAK2 complex fluctuated up to 10 Å, stabilizing at 6 Å. The low RMSD of the pristimerin-JAK2 complex suggests a higher level of stability compared to fedratinib (Fig. 3(a)). Cα RMSD analysis revealed similar RMSD values upon the binding of pristimerin or fedratinib, suggesting that both drugs stabilize the JAK2 protein (Figure 3(b)).

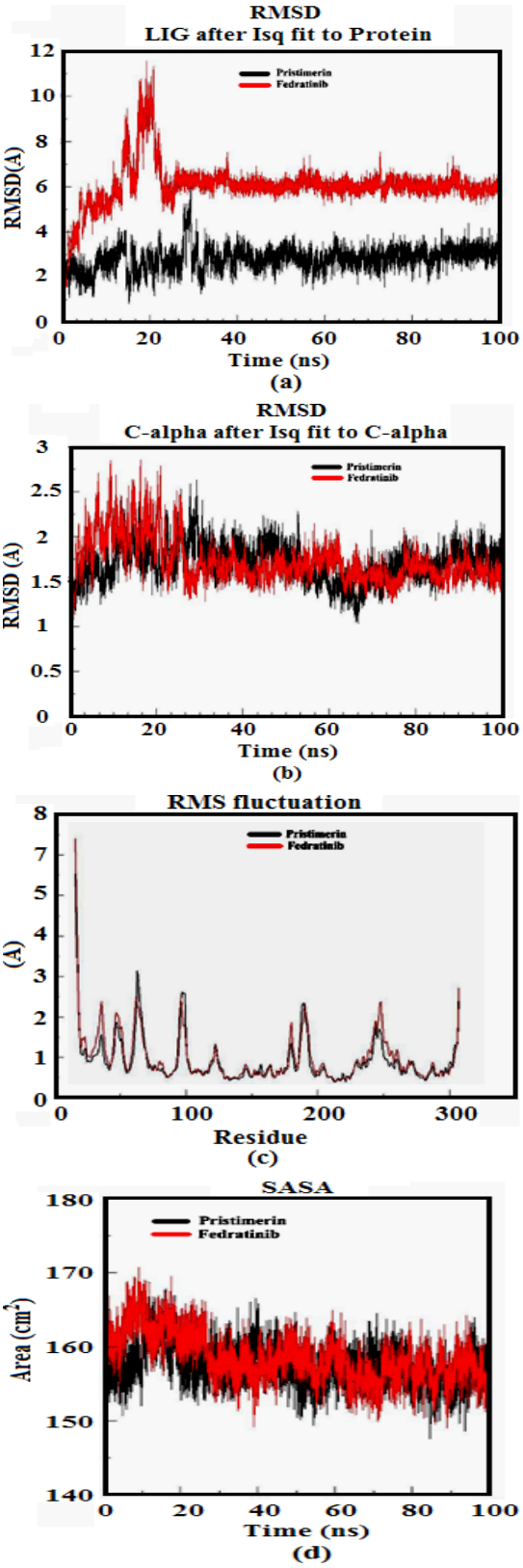

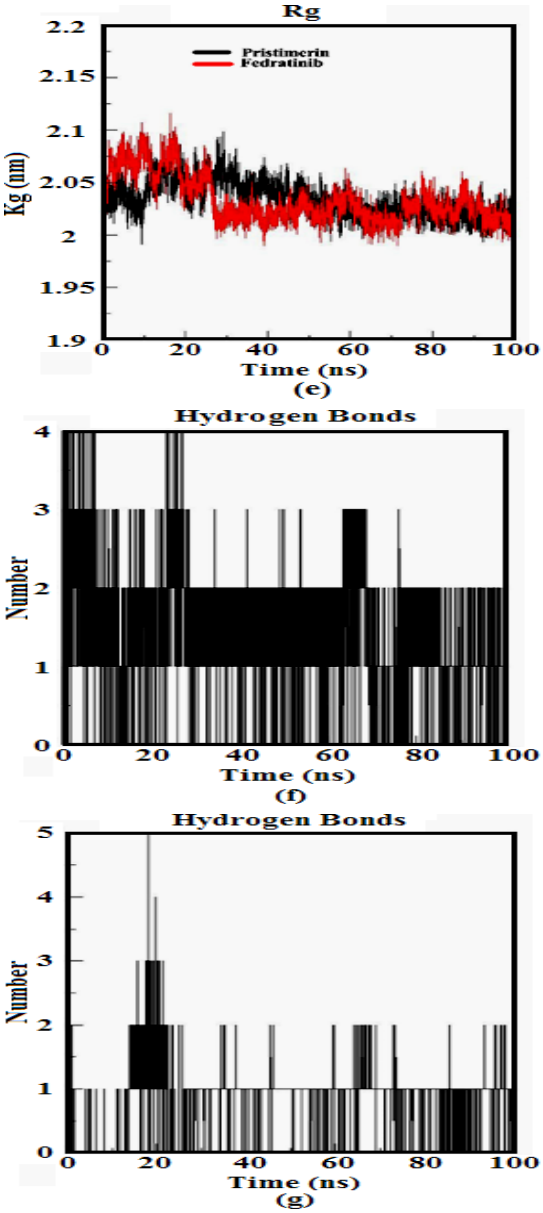

Fig. 3. Changes in (a) RMSD of Pristimerin and the reference JAK2 inhibitor, Fedratinib, complexed with JAK2 protein, (b) RMSD of JAK2 Cα following the binding of the during 100ns of MD simulation (c) RMSF plot per residue for Pristimerin and fedratinib, where (d) represent hydrogen bond formation for pristimerin-JAK2, and (e) represent hydrogen bond formation for Fedratinib-JAK2 during 100ns of molecular dynamic simulation

RMSF analysis indicated that, although the RMSF values for both compounds were similar, fedratinib showed greater fluctuation, particularly at the active site residues Phe860-Val863 and Leu983, which suggests less flexibility at the active site upon pristimerin binding (Fig. 3(c)). Rg analysis of the JAK2 complexes with fedratinib and pristimerin showed similar levels of compactness, with the Rg fluctuating between 2.0-2.1 nm (Fig. 3(e)), and no significant difference in SASA was observed, indicating comparable exposure of both complexes to the solvent.

MD Interaction Analysis

Interaction analysis of the fedratinib-JAK2 complex from the MD trajectory revealed only hydrophobic contacts with Leu855 and Leu884 (Fig. 5(b)). In contrast, pristimerin interacts with JAK2 through a strong hydrogen bond with Arg938 and three weaker hydrogen bonds with Arg938, Asn859, Gly861, and Phe860. Additionally, multiple hydrophobic interactions were observed with Val863 (Fig. 5(a)). A comparison of the docking and MD simulation results demonstrated that the pristimerin-JAK2 interaction remained stable throughout the simulation, with most of the interactions being conserved. Moreover, the hydrogen bond formed by pristimerin showed greater stability during the simulation compared to fedratinib (Figure 3(f) and (g)).

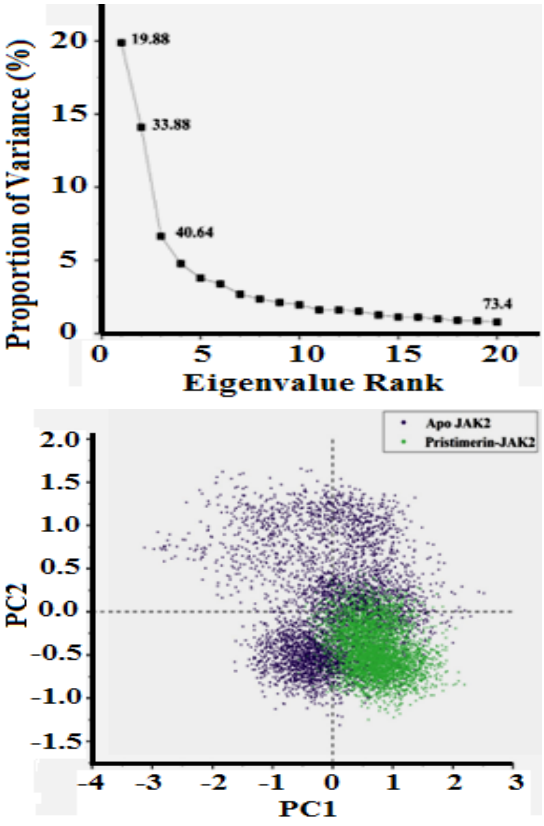

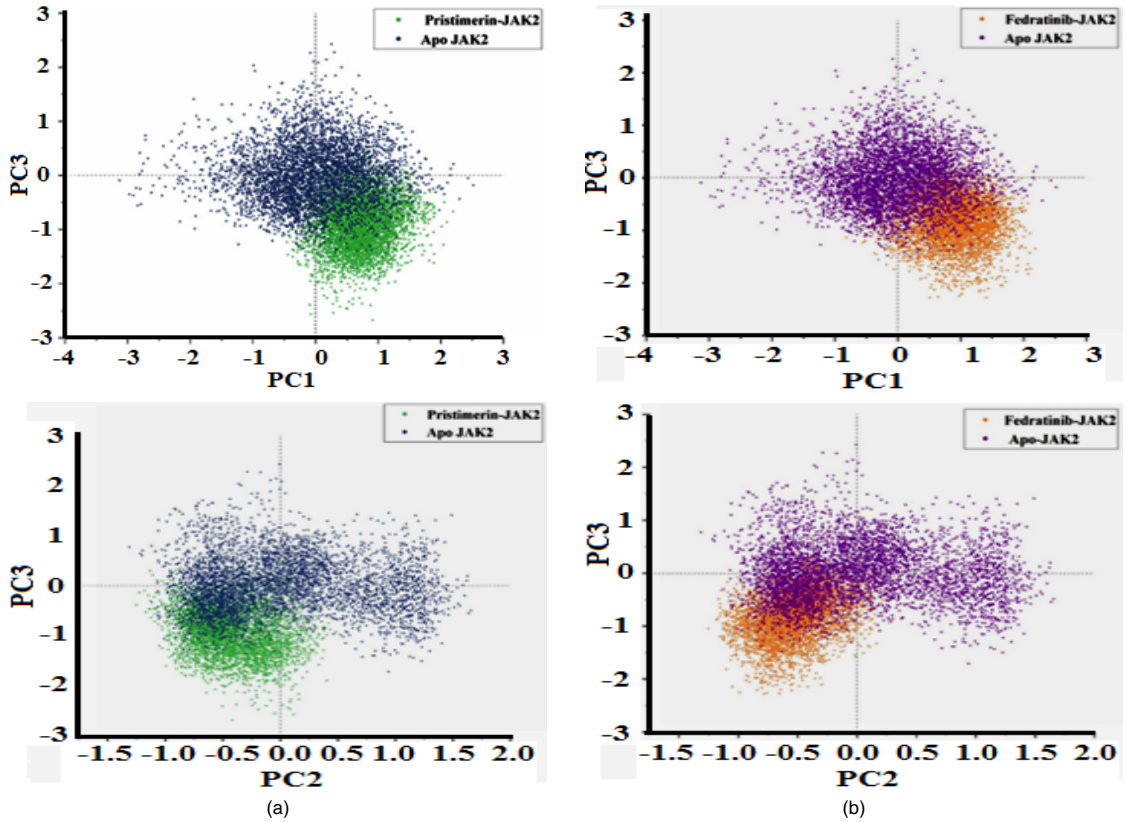

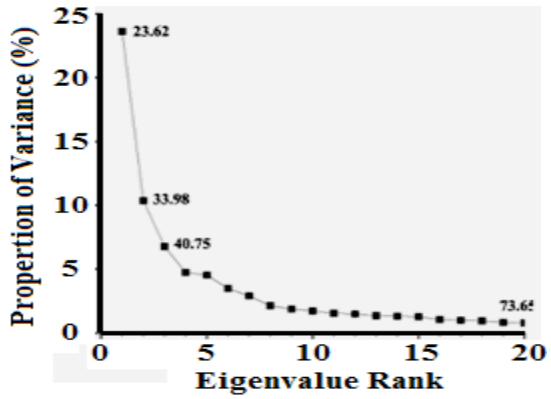

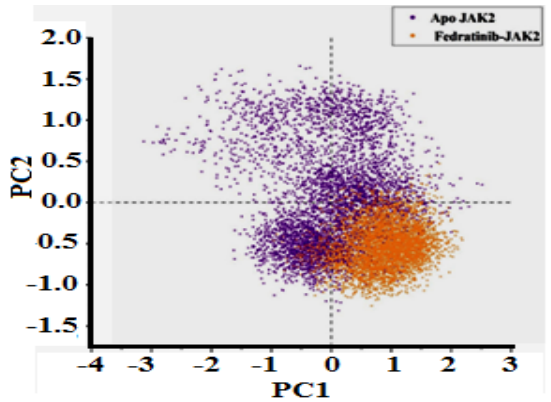

Fig. 4. Principal component demonstrating the proportion of variance for the first 20 Pcs and analysis of Cα collective motion using the first three PCs which highlighted the clustering of the conformation during the last 50 ns of the simulation for (a) Pristimerin and (b) fedratinib

MMPBSA and Decomposition Analysis

The calculated free binding energies for each complex are provided in Table 1. The estimated binding energies indicate that pristimerin exhibits a higher binding affinity for JAK2 compared to fedratinib, as its binding energy is the lowest. This difference can be attributed to the higher contribution of electrostatic interactions to the total binding energy of pristimerin, which is reflected in the greater number of hydrogen bonds formed by pristimerin compared to fedratinib.

Decomposition analysis revealed that Leu855, Val863, and Arg980 contribute most significantly to the binding energy of fedratinib, while Phe860, Val863, and Leu884 are the key residues contributing to the binding energy of pristimerin. Notably, the interaction with Asp994 negatively impacted the binding affinity of both compounds.

Principal Component Analysis (PCA) and Free Energy Landscape (FEL)

To assess the collective motion of the JAK2 inhibitor complexes during the last 50 ns of the simulation, we performed Principal Component Analysis (PCA). The covariance matrix was constructed using the first three principal components (PC1, PC2, and PC3), which explained 40.64% of the total variance in the pristimerin-JAK2 complex and 40.75% of the variance in the fedratinib-JAK2 complex, as shown by the scree plot (Fig. 6). The trace values of the covariance matrix for apo JAK2, pristimerin-JAK2, and fedratinib-JAK2 complexes were 3.09167, 2.81147, and 2.6854 nm², respectively. A slight reduction in trace values suggests a decrease in collective motion and flexibility in the complexes compared to the apo protein.

The change in collective motion was visualized using a 2D projection of PC1, PC2, and PC3 (Fig. 4). Both pristimerin and fedratinib binding reduced the distance between conformations, indicating that JAK2 reached a stable conformation. However, the proportion of variance in PC1 for the pristimerin-JAK2 complex (19.88%) was lower than that for the fedratinib-JAK2 complex (23.62%), suggesting that the pristimerin-JAK2 complex is more stable.

We also evaluated the convergence of the simulations by calculating the cosine content for the eigenvectors of the complexes. The cosine values for PC1 and PC2 were 0.031 and 0.022 for the pristimerin-JAK2 and fedratinib-JAK2 complexes, respectively, indicating good convergence of the simulations during the last 50 ns, thus supporting the suitability of the data for constructing the free energy landscape[48].

Finally, the Free Energy Landscape (FEL) was plotted by correlating the RMSD of the ligand fit to the protein with the radius of gyration to examine and compare the energy minima wells of the JAK2 complexed with pristimerin or fedratinib. While the FEL of the fedratinib-JAK2 complex (Fig. 5(b)) exhibited a more compact energy minima well with a lower free energy for the metastable conformation, a significant number of the conformations did not reach a metastable state. In contrast, most of the pristimerin-JAK2 complex conformations remained within the same energy well, suggesting that the metastable state is easier to attain with pristimerin binding. However, when the fedratinib-JAK2 complex reaches the metastable state, it demonstrates greater stability compared to the pristimerin-JAK2 complex.

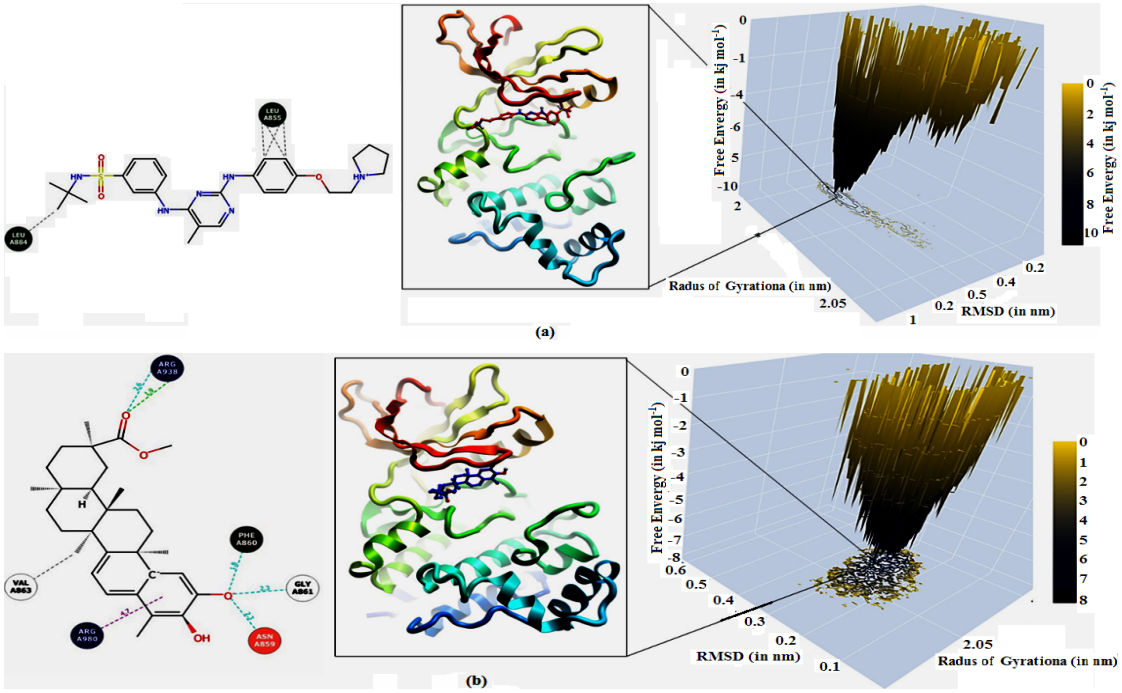

Fig. 5. Gibbs free energy landscape demonstrated the metastable structure when the tested compounds bound to JAK2 during the last 50 ns of the simulation

DISCUSSION

Pristimerin has gained more attention because it has promising clinical options for chemoprevention and treatment of various types of cancer[19,20,49]. The current study was conducted to further explore the anticancer mechanisms of pristimerin on CRC via investigating its activity on the STAT3 signaling pathway. STAT3 plays a significant role in CRC initiation, development, and propagation, and it is considered a cornerstone in CRC hallmarks[9]. Thus, targeting STAT3 signaling pathway is a proposed mechanism for chemoprevention and treatment of CRC[24].

Several structurally related triterpenoids to pristimerin, such as ursolic acid, betulinic acid, and celastrol, were reported to inhibit carcinogenesis of different kinds of cancer partially through suppression of STAT350-52. More in-depth, all of these natural compounds demonstrated an inhibitory action on JAK1 or JAK2 or both[53-55]. Moreover, previous reports proved that pristimerin inhibited the upstream kinases such as P38 or ERK1/2 that contribute to phosphorylation of serine residues in different proteins, including STAT3[56-59]. Meanwhile, our *in vitro* results showed the capability of pristimerin to interfere with STAT3 phosphorylation with dose escalation. These suppressive effects of pristimerin on STAT3 are mediated by inhibition of STAT3-dependent gene expression, including Cyclin D1, Bcl-2, and Bcl-xl[56,60], and might also contribute to synergizing the anticancer activity and reducing chemoresistance of docetaxel in CRC cells[61]. However, these findings do not explain the reduction in the phosphorylated STAT3. Furthermore, pristimerin-induced suppression of STAT3 activation was also reported in prostate cancer cells[62].

The mammalianJAK family comprises four enzymes, namely JAK1, JAK2, JAK3, and TYK2, where JAK1 and JAK2 mediate many functions, such as hematopoiesis, growth, and neural development, while JAK3 and TYK2 function confined to the regulation of the immune response[63]. Thismakes JAK1/2 an interesting target for cancer treatment, and much effort has been made to identify an effective JAK inhibitor. In this study, we further investigated the molecular mechanism behind the inhibitory action of pristimerin on STAT3 phosphorylation at Tyr705 and, eventually, on the activation of STAT3, which was observed in different CRC cells. For that, we used molecular docking and MD simulation to examine the ability of pristimerin to suppress JAK1 and JAK2 kinases in relation to their biological function and implication in cancer development. The Current data suggested that pristimerin might act as a selective JAK2 inhibitor, as the docking scores with JAK1 indicated that pristimerin did not attain the proper pose and affinity to act as an inhibitor for the enzyme, as mentioned earlier.

MD simulation data showed that pristimerin-JAK2 complex demonstrated higher stability as indicated by RMSD data, and in addition to that, the estimated free binding energy of pristimerin indicated that pristimerin has a higher affinity to JAK2 compared to fedratinib as a result of the higher rate of hydrogen bond formation. Furthermore, analysis of the Cα fluctuation during the last 50 ns of the simulation using principal component analysis demonstrated the ability of pristimerin to reduce the collective motion of the JAK2 kinase domain and forced the protein to attain conformations with a lower energy, which indicated the stability of the complex.

The above facts indicate that pristimerin can act as a selective JAK2 inhibitor, which might explain the reduced level of phosphorylated STAT3 in HCT-116 cells that were treated with pristimerin. Therefore, pristimerin as a lead compound might prevail over the successor's selective JAK2 inhibitor as an anti-cancer for solid tumors, adding to that the ability of pristimerin to target multiple pathways involved in carcinogenesis, including MAPK[64], PI3K/AKT/mTOR[65], Wnt/β-Catenin[66], and NF-κB pathway[20]. This reflects its diverse antitumor effects, including apoptosis induction, autophagy induction, inhibition of metastasis and angiogenesis, and synergistic effect with other chemotherapeutic agents[19,49]. Also, the current data might encourage the assessment of pristimerin as a possible chemotherapeutic against hematological malignancies, in particular, Myelogenous neoplasm, as indicated for JAK2 inhibitors.

CONCLUSION

Our *in silico* and *in vitro* results suggested that pristimerin displays its anticancer effect on colorectal cancer through inhibition of STAT3 activation in HCT-116 cells. STAT3 signaling

pathway represents an important molecular target for pristimerin anticancer activities.

ACKNOWLEDGEMENT

Not applicable

Availability of Data and Materials

The datasets supporting the findings of the current study are openly available athttps://zenodo.org/ at doi: 10.5281/zenodo.13893596

Conflict of interests

The authors declare no conflicts of interest relevant to the content of this article.

Funding/Support

This research did not receive any specific grant from funding agencies in the public, commercial, or not-for-profit sectors.

REFERENCES

1. Xi, Y.; Xu, P., *Transl. Oncol.*, **2021**, *14*(6), 101174. doi:10.1016/j.tranon.2021.101174.
2. Rawla, P.; Sunkara, T.; Barsouk, A., *Prz. Gastroenterol.*, **2019**, *14*(2), 89–103.doi: 10.5114/pg.2018.81072.
3. Ahadi, M.; Sokolova, A.; Brown, I.; Chou, A.; Gill, A. J., *Pathology*, **2021**, *53*(4), 454–461. doi: 10.1016/j.pathol.2020.10.010.
4. Alzahrani, S. M.; Al Doghaither, H. A.; Al-Ghafari, A. B., *Mol. Clin. Oncol.*, **2021**, *15*(3), 271. doi:10.3892/mco.2021.2433.
5. Nguyen, H. T.; Duong, H. Q., *Oncol. Lett.,* **2018**, *16*(1), 9–18.doi:10.3892/ol.2018.8679.
6. Tsareva, S. A.; Moriggl, R.; Corvinus, F. M.; Wiederanders, B.; Schütz, A.; Kovacic, B., *Neoplasia.*, **2007**, *9*(4), 279–291.doi:10.1593/neo.06820.
7. Malki, A.; ElRuz, R. A.; Gupta, I.; Allouch, A.; Vranic, S.; Al Moustafa, A. E., *Int. J. Mol. Sci.,* **2020**, *22*(1), 130. doi:10.3390/ijms22010130.
8. Xiong, H.; Zhang, Z. G.; Tian, X. Q.; Sun, D. F.; Liang, Q. C.; Zhang, Y. J., *Neoplasia.*, **2008**, *10*(3), 287–297.doi:10.1593/neo.07971.
9. Gao, P.; Niu, N.; Wei, T.; Tozawa, H.; Chen, X.; Zhang, C., *Oncotarget*, **2017**, *8*(41), 69139–69161. doi:10.18632/oncotarget.20360.
10. Wendt, M. K.; Balanis, N.; Carlin, C. R.; Schiemann, W. P., *JAK-STAT.*, **2014**, *3*(1), e28975. doi: 10.4161/jkst.28975.
11. Rébé, C.; Ghiringhelli, F., *Cancers (Basel).,* **2019**, *11*(9), 1280.doi:10.3390/cancers11091280.
12. Wang, Q.; Shen, X.; Chen, G.; Du, J., *Cancers (Basel).,* **2022**, *14*(12), 2928.doi:10.3390/cancers14122928.
13. Kwon, G. T.; Jung, J. I.; Song, H. R.; Woo, E. Y.; Jun, J. G.; Kim, J. K., *J. Nutr. Biochem.*, **2012**, *23*(3), 228–238.doi:10.1016/j.jnutbio.2010.11.019.
14. Zhuang, S., *Cell Signal.,* **2013**, *25*(9), 1924–1931. doi: 10.1016/j.cellsig.2013.05.007.
15. Dong, J.; Cheng, X. D.; Zhang, W. D.; Qin, J. J., *J. Med. Chem.*, **2021**, *64*(13), 8884–8915. doi: 10.1021/acs.jmedchem.1c00629.
16. Dehelean, C. A.; Marcovici, I.; Soica, C.; Mioc, M.; Coricovac, D.; Iurciuc, S., *Molecules.*, **2021**, *26*(4), 1109. doi:10.3390/molecules26041109.
17. Brinker, A. M.; Ma, J.; Lipsky, P. E.; Raskin, I., *Phytochemistry.*, **2007**, *68*(6), 732–766.doi: 10.1016/j.phytochem.2006.11.029.
18. Dirsch, V. M.; Kiemer, A. K.; Wagner, H.; Vollmar, A. M., *Eur. J. Pharmacol.,* **1997**, *336*(2-3), 211–217.doi: 10.1016/S0014-2999(97)01245-4.
19. Li, J. J.; Yan, Y. Y.; Sun, H. M.; Liu, Y.; Su, C. Y.; Chen, H. B., *Front. Pharmacol.*, **2019**, *10*, 746. doi:10.3389/fphar.2019.00746.
20. Yousef, B. A.; Hassan, H. M.; Zhang, L. Y.; Jiang, Z. Z., *Curr. Cancer Drug Targets.*, **2017**, *17*(1), 100–108. doi:10.2174/1568009616666160112105824.
21. Yousef, B. A.; Hassan, H. M.; Zhang, L. Y.; Jiang, Z. Z., *Phytomedicine.*, **2018**, *40*(2), 140–147. doi: 10.1016/j.phymed.2018.01.008.
22. Park, J. H.; Kim, J. K., *Phytomedicine.*, **2018**, *42*(1), 164–171.doi:10.1016/j.phymed.2018.03.033.
23. Zhao, Q.; Bi, Y.; Guo, J.; Liu, Y.; Zhong, J.; Pan, L., *Phytomedicine.*, **2021**, *80*(3), 153399.doi: 10.1016/j.phymed.2020.153399.
24. Gargalionis, A. N.; Papavassiliou, K. A.; Papavassiliou, A.G., *Biomedicines.*, **2021**, *9*(8), 1016. doi: 10.3390/biomedicines9081016.
25. Cheeseright, T.; Mackey, M.; Rose, S.; Vinter, A., *J. Chem. Inf. Model.*, **2006**, *46*(2), 665–676. doi:10.1021/ci050357s.

26. Bauer, M. R.; Mackey, M. D., *J. Med. Chem.*, **2019**, *62*(7), 3036–3050.doi:10.1021/acs.jmedchem.8b01925.
27. Kuhn, M.; Firth-Clark, S.; Tosco, P.; Mey, A.; Mackey, M.; Michel, J., *J. Chem. Inf. Model.*, **2020**, *60*(6), 3120–3130.doi:10.1021/acs.jcim.0c00165.
28. Pronk, S.; Pall, S.; Schulz, R.; Larsson, P.; Bjelkmar, P.; Apostolov, R., *Bioinformatics.*, **2013**, *29*(7), 845–854.doi:10.1093/bioinformatics/btt055.
29. Vasbinder, M. M.; Alimzhanov, M.; Augustin, M.; Bebernitz, G.; Bell, K.; Chuaqui, C., *Bioorg. Med. Chem. Lett.*, **2016**, *26*(1), 60–67. doi: 10.1016/j.bmcl.2015.11.031.
30. Davis, R. R.; Li, B.; Yun, S. Y.; Chan, A.; Nareddy, P.; Gunawan, S., *J. Med. Chem.*, **2021**, *64*(4), 2228–2241.doi:10.1021/acs.jmedchem.0c01952.
31. Bernstein, F. C.; Koetzle, T. F.; Williams, G. J.; Meyer, E. F., Jr.; Brice, M. D.; Rodgers, J. R., *Arch. Biochem. Biophys.*,**1978**, *185*(2), 584–591.doi:10.1016/S0022-2836(77)80200-3.
32. Waterhouse, A.; Bertoni, M.; Bienert, S.; Studer, G.; Tauriello, G.; Gumienny, R., *Nucleic Acids Res.*, **2018**, *46*(W1), W296–W303. doi: 10.1093/nar/gky427.
33. Pettersen, E. F.; Goddard, T. D.; Huang, C. C.; Couch, G. S.; Greenblatt, D. M.; Meng, E. C., *J. Comput. Chem.*, **2004**, *25*(13), 1605–1612. doi: 10.1002/jcc.20084.
34. Zoete, V.; Cuendet, M. A.; Grosdidier, A.; Michielin, O., *J. Comput. Chem.*, **2011**, *32*(11), 2359–2368.doi:10.1002/jcc.21816.
35. Valdes-Tresanco, M. S.; Valdes-Tresanco, M. E.; Valiente, P. A.; Moreno, E., *J. Chem. Theory Comput.*, **2021**, *17*(10), 6281–6291. doi: 10.1021/acs.jctc.1c00645.
36. Miller, B. R.; III; McGee, T. D.; Jr.; Swails, J. M.; Homeyer, N.; Gohlke, H.; Roitberg, A. E., *J. Chem. Theory Comput.*, **2012**, *8*(9), 3314–3321. doi: 10.1021/ct300418h.
37. Baker, N. A.; Sept, D.; Joseph, S.; Holst, M. J.; McCammon, J. A., *Proc. Natl. Acad. Sci.*, U.S.A., **2001**, *98*(18), 10037–10041.doi: 10.1073/pnas.181342398.
38. Gohlke, H.; Kiel, C.; Case, D. A., *J. Mol. Biol.*, **2003**, *330*(4), 891–913. doi:10.1016/S0022-2836(03)00610-7.
39. Amadei, A.; Linssen, A. B.; Berendsen, H. J., *Proteins.*, **1993**, *17*(4), 412–425. doi:10.1002/prot.340170408.
40. de Groot, B. L.; Amadei, A.; Scheek, R. M.; van Nuland, N. A.; Berendsen, H. J., *Proteins.*, **1996**, *26*(3), 314–322. doi:10.1002/(SICI)1097-0134(199611)26:3<314::AID-PROT7>3.0.CO;2-D.
41. Kitao, A.; Go, N., *Curr. Opin. Struct. Biol.*, **1999**, *9*(2), 164–169.doi:10.1016/S0959-440X(99)80023-2.
42. Berendsen, H. J.; Hayward, S., *Curr. Opin. Struct. Biol.*, **2000**, *10*(2), 165–169.doi: 10.1016/S0959-440X(00)00061-0.
43. Stroganov, O. V.; Novikov, F. N.; Stroylov, V. S.; Kulkov, V.; Chilov, G. G., *J. Chem. Inf. Model.*, **2008**, *48*(12), 2371–2385.doi:10.1021/ci800166p.
44. Novikov, F. N.; Stroylov, V. S.; Zeifman, A. A.; Stroganov, O. V.; Kulkov, V.; Chilov, G. G., *J. Comput.-Aided Mol. Des.*, **2012**, *26*(7), 725–735. doi:10.1007/s10822-012-9549-y.
45. Hollingsworth, S. A.; Dror, R. O., *Neuron.*, **2018**, *99*(6), 1129–1143.doi:10.1016/j.neuron.2018.08.011.
46. Huang, X.; Powers, R., *J. Am. Chem. Soc.*, **2001**, *123*(16), 3834–3835.doi:10.1021/ja005770p.
47. Lee, B.; Richards, F. M., *J. Mol. Biol.,* **1971**, *55*(3), 379–400.doi:10.1016/0022-2836(71)90324-x.
48. Maisuradze, G. G.; Leitner, D. M., *Proteins.*, **2007**, *67*(3), 569–578.doi:10.1002/prot.21344.
49. Wang, Y.; Feng, W.; Wang, X.; Li, X.; Mou, Y.; Zhang, Y., *Biomed. Pharmacother.,* **2022**, *154*, 113575.doi:10.1016/j.biopha.2022.113575.
50. Liu, T.; Ma, H.; Shi, W.; Duan, J.; Wang, Y.; Zhang, C., *Int. J. Oncol.*, **2017**, *51*(2), 555–562.doi:10.3892/ijo.2017.4035.
51. Su, D.; Gao, Y. Q.; Dai, W. B.; Hu, Y.; Wu, Y. F.; Mei, Q. X., Evid.-Based Complement. *Alternat. Med.*, **2017**, *2017*, 5180707.doi: 10.1155/2017/5180707.
52. Zhao, Z.; Wang, Y.; Gong, Y.; Wang, X.; Zhang, L.; Zhao, H., *J. Transl. Med.*, **2022**, *20*(1), 525. doi:10.1186/s12967-022-03741-9.
53. Pathak, A. K.; Bhutani, M.; Nair, A. S.; Ahn, K. S.; Chakraborty, A.; Kadara, H., *Mol. Cancer Res.*, **2007**, *5*(9), 943–955.doi: 10.1158/1541-7786.MCR-06-0348.

54. Rajendran, P.; Li, F.; Shanmugam, M. K.; Kannaiyan, R.; Goh, J. N.; Wong, K. F., *Cancer Prev. Res. (Phila).,* **2012**, *5*(5), 631–643.doi: 10.1158/1940-6207.CAPR-11-0420.
55. Pandey, M. K.; Sung, B.; Aggarwal, B. B., *Int. J. Cancer.*, **2010**, *127*(2), 282–292.doi: 10.1002/ijc.25059.
56. Yousef, B. A.; Guerram, M.; Hassan, H. M.; Hamdi, A. M.; Zhang, L. Y.; Jiang, Z. Z., *Oncol. Rep.*, **2016**, *35*(2), 1091–1100. doi:10.3892/or.2015.4457.
57. Yan, Y. Y.; Bai, J. P.; Xie, Y.; Yu, J. Z.; Ma, C. G., *Oncol. Lett.,* **2013**, *5*(1), 242–248.doi: 10.3892/ol.2012.982.
58. Yousef, B. A.; Hassan, H. M.; Guerram, M.; Hamdi, A. M.; Wang, B.; Zhang, L. Y., *Biomed. Pharmacother.*, **2016**, *79*(1), 112–119.doi: 10.1016/j.biopha.2016.02.003.
59. Byun, J. Y.; Kim, M. J.; Eum, D. Y.; Yoon, C. H.; Seo, W. D.; Park, K. H., *Mol. Pharmacol.*, **2009**, *76*(4), 734–744.doi:10.1124/mol.109.056259.
60. Wang, Y.; Zhou, Y.; Zhou, H.; Jia, G.; Liu, J.; Han, B., *PLoS One.*, **2012**, *7*(8), e43826. doi: 10.1371/journal.pone.0043826.
61. Yousef, B. A.; Hassan, H. M.; Elhafiz, M.; Zhang, L.; Jiang, Z., *Synergy.*, **2020**, *11*, 100068. doi: 10.1016/j.synres.2020.100068.
62. Liu, Y. B.; Gao, X.; Deeb, D.; Pindolia, K.; Gautam, S. C., *J. Exp. Ther. Oncol.*, **2015**, *11*(1), 41–49.
63. O'Shea, J. J.; Holland, S. M.; Staudt, L. M., N., *Engl. J. Med.*, **2013**, *368*(2), 161–170. doi: 10.1056/NEJMra1202117.
64. Lee, Y.; Na, J.; Lee, M. S.; Cha, E. Y.; Sul, J. Y.; Park, J. B., *Mol. Med. Rep.*, **2018**, *18*(5), 4281–4288. doi: 10.3892/mmr.2018.9488.
65. Deeb, D.; Gao, X.; Liu, Y. B.; Pindolia, K.; Gautam, S. C., *Int. J. Oncol.,* **2014**, *44*(5), 1707–1715. doi: 10.3892/ijo.2014.2325.
66. Cevatemre, B.; Erkisa, M.; Aztopal, N.; Karakas, D.; Alper, P.; Tsimplouli, C., *Pharmacol. Res.*, **2018**, *129*(3), 500–514.0doi:10.1016/j.phrs.2017.11.027.